Kr-based buffer gas for Rb vapor-cell clocks

Kr-based buffer gas for Rb vapor-cell clocks

Michele Gozzelino, Salvatore Micalizio, Claudio E. Calosso, Aldo Godone, and Filippo Levi

Optically pumped Rb vapor cell clocks are by far the most used devices for timekeeping in all ground and space applications. The compactness and the robustness of this technology make Rb clocks extremely well fit to a large number of applications including GNSS, telecommunication and network synchronization. Many efforts are devoted to improve the stability of Rb clocks and reduce their environmental sensitivity.

In this paper, we investigate the use of a novel mixture of buffer gas based on Kr and $\mathbf{N_2}$, capable of reducing by more than one order of magnitude the barometric and temperature sensitivities of the clock, with possible improvement of their long-term stability.

I. Introduction

In Rb optically pumped clocks a buffer gas (BG) is added to the evacuated Rb cell to avoid inelastic collisions with the cell's wall. Gas collisions with Rb vapor should be as much as possible non-perturbing, to minimize the effect on Rb coherence and population inversion relaxation rates. When the BG pressure is sufficiently high, the mean free path of the Rb atom is strongly reduced and its trajectory is a random walk, confining thus Rb atoms in a much smaller volume of the cell. However, all BGs produce a shift of the clock transition (and of the optical transitions as well), that is a function of the gas pressure and temperature.

Many BGs were studied in the past: light gases as He, Ne, N_2 are known to produce positive shifts, whereas heavier gases like Ar, Kr produce a negative shift (see [1] and references therein). The BG pressure shift, for a sealed cell, is a function of the cell temperature: neglecting higher-order term, this shift can be expressed as:

$$\nu(P, \Delta T) = \nu_0 + P\left(\beta + \delta\Delta T + \gamma\Delta T^2\right) \tag{1}$$

where ν_0 is the Rb unperturbed clock transition frequency, P is the BG pressure inside the cell, β, δ and γ are parameters characterizing the specific BG and ΔT is the temperature variation with respect to an arbitrary working point T_0. In Eq. (1) we remind that P is given by $P = nk_BT_s$, where n is the buffer gas number density, k_B is the Boltzmann constant and T_s is the cell temperature at time of sealing. The buffer gas induced shift is then more properly described as a density or collisional shift.

When a mixture of two gases with a pressure ratio r is used, we can write eq. (1) for each gas and perform a linear combination of the contributions, obtaining:

$$\nu(P_t, \Delta T) = \nu_0 + P_t\left(\beta' + \delta'\Delta T + \gamma'\Delta T^2\right) \tag{2}$$

Authors are with Istituto Nazionale di Ricerca Metrologica, INRIM, Torino, Italy.
E-mail: s.micalizio@inrim.it

Table I: Buffer gas coefficients for Ar, N_2, Kr and Ne of the 0-0 hyperfine transition of ^{87}Rb for a vapor temperature $T_0 \simeq 333\,\mathrm{K}$. The reported coefficients are the average of the values available from [3–8]. The uncertainty is set as the scatter between the published values. In the case of the γ coefficient, a value for Ar and N_2 is reported only in [3] and no uncertainty is provided.

	Ar	**N_2**	**Kr**	**Ne**
$\boldsymbol{\beta}$ **/(Hz/Torr)**	-62(7)	550(10)	-610(10)	380(30)
$\boldsymbol{\delta}$ **/(Hz/Torr/K)**	-0.34(4)	0.54(2)	-0.63(2)	0.19(8)
$\boldsymbol{\gamma}$ **/(Hz/Torr/K^2)**	-0.00035	-0.0015	–	–

where P_t is the total pressure of the gas mixture and β' is given as:

$$\beta' = \frac{\beta_1 + r\beta_2}{1 + r}. \tag{3}$$

where β_1 and β_2 are the coefficients of the BGs composing the mixture. Analogous expressions are valid for δ' and γ'.

To reduce the dependence of the BG shift on temperature, a mixture of Ar and N_2 gases is widely used [1]. Since these two gases have δ parameters with opposite sign, it is possible to zero the δ' term, producing a quadratic temperature sensitivity for the Rb hyperfine frequency transition. Typically, the clock works at the vertex of the resulting parabola, in a minimum of the temperature sensitivity function. In a well-engineered system, the BG mixture is chosen to have the vertex of the parabola at the desired temperature, where the Rb density is optimal with respect to other physical parameters (such as cell length, optical pumping power, etc).

In the literature, a large number of experimental data can be found reporting β and δ for the most commonly used buffer gases, Ar and N_2 over all. In particular, N_2 is very often used in Rb clocks for his properties of fluorescence quenching [2]. In fact, during the optical pumping process, the inelastic collisions of Rb atoms in the excited state with N_2 molecules result in a non-radiative decay of Rb to the ground state with a significant branching ratio. Fluorescence quenching reduces by more than one order of magnitude the number of spontaneous decay emitted photons that counteract the optical pumping process. In table I the β, γ and δ coefficients are presented for different buffer gases of interest for clock applications.

It is evident that a mixture of Ar and N_2 aimed for a reduction of the δ' parameter results in a large β'. This has two main effects:

1) Linear sensitivity of the clock frequency to barometric fluctuations. A variation of the environmental pressure P_{out} produces a deformation of the glass cell, that

induces a variation of the cell's volume and consequently of the inner BG pressure P_t. This results in a pressure sensitivity of the clock transition frequency ν:

$$\frac{\Delta\nu}{\Delta P_{out}} = \frac{\partial\nu}{\partial P_t}\frac{\Delta P_t}{\Delta P_{out}} \simeq \beta' \frac{\Delta P_t}{\Delta P_{out}} \tag{4}$$

The relation $\frac{\Delta P_t}{\Delta P_{out}}$ is a coefficient that depends only on geometrical and material properties, thus the barometric sensitivity of the clock frequency is proportional to β' [9,10]. In laboratory experiment, for a borosilicate cell and a traditional Ar-N_2 mixture, we have measured a sensitivity coefficient of $\simeq 7\times10^{-16}\,\mathrm{Pa}^{-1}$. During bad weather conditions, atmospheric pressure can drop even more than 300 Pa in a few hours, resulting in a fractional frequency shift larger than 2×10^{-13}. A similar coefficient was measured in [11], where the physics package was placed in a hermetic chamber to make the barometric shift negligible.

2) Linear sensitivity of the clock frequency to temperature gradients variations. If the Rb cell suffers from a time-varying temperature gradient, this results in a variation of the local density of the BG in the active volume, producing a frequency shift of the clock transition. It is worth noting that a gradient in the Rb cell is often desirable and many clocks are engineered to have a Rb reservoir outside the cavity volume at a lower temperature. As discussed in [12], for a cell with the main body at temperature T_0 and a reservoir at temperature T_b, the sensitivity to a variation of the temperature difference $(T_0 - T_b)$ can be expressed as:

$$\frac{\Delta\nu}{\Delta(T_0 - T_b)} \simeq -\frac{P_t\beta' v_b}{T_b} \tag{5}$$

where v_b is the ratio between the volume of the cell at temperature T_b and the total cell volume. Thus, also this effect can be mitigated by lowering the coefficient β', relaxing the specifications on the cell temperature stabilization. Equation (5) is derived and experimentally verified in [12].

According to the values reported in table II, we can see that a mixture of N_2 and Kr can reduce the δ' and β' parameters at the same time, resulting in a strong mitigation of the aforementioned sensitivities.

Equation (1) implies a linear shift of the clock frequency with respect to pressure. This is verified for light noble gases such as Ne and Ar. For heavier noble gases, 3-bodies interactions, and in particular the creation of Van der Waals molecules, introduce a departure from the strictly linear behavior [13–15]. Nevertheless, the non-linear shift contribution for Kr is limited to a few tens of Hz for typical pressures ($P_{Kr} \leq 20$ Torr), whereas the absolute shift induced by an Ar-N_2 mixture usually is of a few kHz [12]. A significant reduction of the total BG shift can thus be reached with a proper mixture of Kr and N_2.

Another consequence of Van der Waals molecules is the augmented relaxation rates [1,16]. For the population relaxation rates, we expect a contribution $\gamma_1^* \simeq 350\,\mathrm{s}^{-1}$ coming solely from the Kr-Rb collisions, mostly independent from the BG pressure (for $P_{Kr} > 10$ Torr), while the contribution to the transverse relaxation be as high as $\gamma_2^* = 1400\,\mathrm{s}^{-1}$.

Table II: Buffer gas coefficients for the Ar-N_2 and Kr-N_2 mixtures described in the text for the 0-0 hyperfine transition of ^{87}Rb for a vapor temperature $T_0 \simeq 333$ K. The values of the coefficients for the single buffer gases are taken from table I. For the Ar-N_2 mixture there is good agreement with the data reported in [12] and [17].

	Ar-N_2 (1.6:1)	**Kr-N_2 (0.9:1)**
β' **/(Hz/torr)**	175(6)	3(8)
δ' **/(Hz/torr/K)**	-0.00(2)	-0.01(1)
γ' **/(Hz/torr/K^2)**	-0.0008	–

Despite the expected higher relaxation rates, we have estimated that a mixture of Kr and N_2 can be of interest, since the short term Allan deviation can still be $\sigma_y(\tau) < 1\times10^{-12}\,\tau^{-1/2}$, with a significant reduction of the environmental sensitivities above discussed. This is particularly true for those applications where long-term stability in an uncontrolled environment is the main concern.

In the next section we discuss the results obtained with a cell containing a mixture of Kr and N_2, using a compact Rb pulsed optically pumped clock (POP) as a test-bed. Specifically, we provide a characterization of the cell parameters in the clock setup, including relaxation coefficients, Ramsey fringes observation and preliminary frequency stability measurement.

II. Experimental setup and results

The clock cell under test is made of Pyrex and filled with a mixture of Kr and N_2 (ratio 0.96). As a term of comparison, a second cell (with identical volume and made of fused silica) was filled with a more standard Ar-N_2 mixture (ratio 1.6).

Our experiment is based on the POP idea, where optical pumping, microwave excitation and detection are separated in time. A schematic of the set-up is depicted in Fig. 1, a more detailed description of a POP clock can be found in [18].

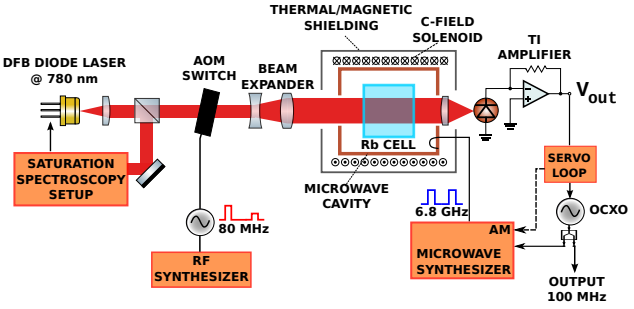

Figure 1: Sketch of the POP clock experimental setup.

A laser diode tuned on the Rb D_2 transition is frequency locked to a reference cell containing only ^{87}Rb with a saturation spectroscopy scheme. The main laser path is then frequency shifted by an acoustooptic modulator (AOM), expanded and sent to the Rb clock cell. The frequency of the

AOM and the reference sub-Doppler Lamb dip are chosen to tune the laser on the minimum of the absorption profile for the clock cell containing the BG mixture. The BG shift on the D_2 optical transition is found to be $-310\,\mathrm{MHz}$ for the Kr-N_2 mixture, corresponding to a linear pressure coefficient of $-7.7\,\mathrm{MHz/Torr}$, in reasonable agreement with the values reported in the literature [19,20].

The AOM transmission is digitally controlled to create the pumping and detection pulses and switched off during the Ramsey interrogation time (T_R). Typically, the pumping power can be as high as $10\,\mathrm{mW}$, whereas the detection power is $\simeq 200\,\mu\mathrm{W}$, for a beam waist of $\simeq 6\,\mathrm{mm}$.

A low-noise quartz oscillator is frequency multiplied to $6.8\,\mathrm{GHz}$. The exact Rb frequency is reached mixing this signal with a signal generated by a direct digital synthesizer (DDS) tuned at $34.7\,\mathrm{MHz}$. The amplitude of the DDS output is modulated to generate the two Ramsey pulses [21,22].

The Rb vapor cell is cylindrical with an internal diameter of $1\,\mathrm{cm}$ and $1\,\mathrm{cm}$ long. It is contained in low-Q (around 1000) loaded microwave cavity resonant on the TE_{011} mode. The cavity-cell assembly is temperature stabilized to better than 5 mK and placed inside a magnetically shielded environment. A photodiode detects the absorption of the probe laser pulse as the microwave frequency is dithered, providing the clock signal. The pattern generator and the signal acquisition are handled by a low-noise digital electronic system [23].

The POP clock is quite well suited to study the relaxation rates of the atomic population: in fact, we can easily change the Ramsey time duration and measure the variation of the central fringe contrast (which is related to the atomic coherence relaxation), or we can delay the microwave interrogation after the optical pumping pulse to measure the population inversion relaxation. A sketch of the basic POP interrogation sequence is depicted in Fig. 2. The whole cycle lasts a few ms, corresponding to a modulation frequency in the range $100\,\mathrm{Hz}$ to $300\,\mathrm{Hz}$.

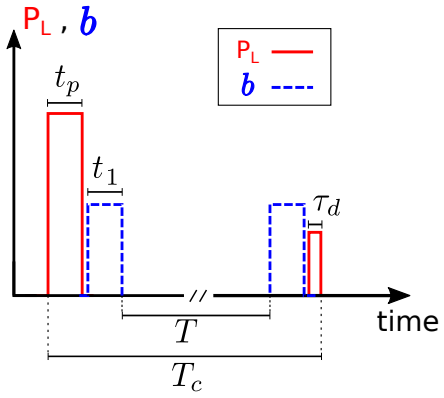

Figure 2: POP basic sequence. P_L stands for laser power, while b is the microwave Rabi frequency (proportional to the amplitude of the pulses). The free-evolution time T is in the range $1\,\mathrm{ms}$ to $5\,\mathrm{ms}$ for typical working conditions. The Rabi pulses duration t_1 is set to be $\simeq 0.1\,T$, the pumping time t_p is $< 0.5\,\mathrm{ms}$ and the detection time $\tau_d \simeq 150\,\mu\mathrm{s}$.

To evaluate the BG performance, the first characterization is to measure the frequency-versus-temperature dependence. We have performed such an experiment with a Kr-N_2 cell and with a Ar-N_2 cell sealed at a nominal pressure of 40 Torr and 50 Torr, respectively. The two sets of frequency measurements are shown in Fig. 3. The frequency data are fitted with Equation (2), close to the BG's inversion point, to retrieve the values of β' and γ' (δ' is routinely set to zero for small temperature offsets from the shift inversion point). With this procedure, for the Ar-N_2 cell, a quadratic temperature coefficient $\gamma' = -1.0(1) \times 10^{-3}\,\mathrm{Hz\,K^{-2}Torr^{-1}}$ is obtained; in the Kr-N_2 cell, instead, we have measured $-0.9(1) \times 10^{-3}\,\mathrm{Hz\,K^{-2}Torr^{-1}}$. To our knowledge, the value of γ' was not measured before for a Kr-N_2 mixture.

The most relevant information for the current investigation is the absolute frequency value of the parabola's vertex with respect to the unperturbed clock transition. This corresponds to the total BG shift $\Delta\nu_0 = \beta' P_t$ and it is measured to be: $\Delta\nu_0 = -407(5)\,\mathrm{Hz}$ for the Kr-N_2 cell, and $\Delta\nu_0 = 8517(10)\,\mathrm{Hz}$ for the Ar-N_2 cell. Assuming the nominal sealing pressure P_t as known, we can retrieve $\beta' = -10(1)\,\mathrm{Hz\,Torr^{-1}}$ for this particular Kr-N_2 mixture. This corresponds to a reduction of a factor 17 of the β' parameter with respect to an Ar-N_2 system, directly impacting on barometric and anomalous temperature sensitivities.

From the coefficient values present in the literature and the newly available data of this work, we estimated that a Kr-N_2 mixture with 0.92 ratio will further reduce the absolute shift and slightly move the vertex of the parabola towards higher temperatures. Such a refined mixture will be experimentally investigated in future works, possibly at different total BG pressures, to corroborate the shift estimate and to find the optimal total pressure for centimeter-scale clock cells.

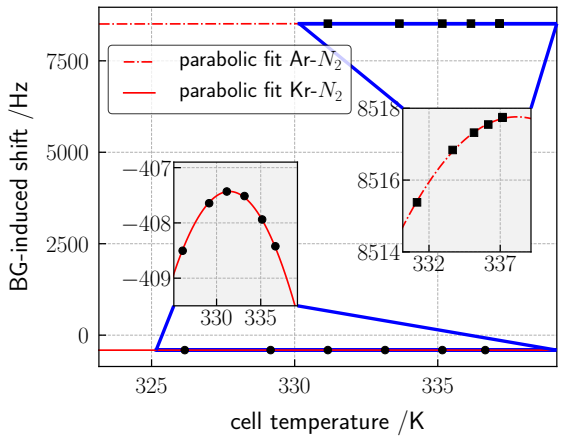

Figure 3: Absolute frequency shift induced by the buffer gas with respect to the unperturbed $^{87}\mathrm{Rb}$ clock transition for the two buffer gas mixtures described in the text. The insets show a zoom of the frequency measurement around the inversion point, highlighting the quadratic behavior.

To estimate the population inversion relaxation time (T_1) we used the well-known Franzen method [24,25], where in

absence of microwave excitation, a tunable dark time (T_{dark}) is inserted between the pumping pulse and a probe pulse. After the pumping pulse, as the atomic population imbalance decays, the transmitted optical power during the probe pulse changes accordingly. The transmission signal can thus be described with the following best-fit function:

$$A + B \exp\left\{-\frac{T_{dark}}{T_1}\right\} \tag{6}$$

The value of T_1 depends on temperature, mainly through the Rb atomic density that introduces a spin-exchange relaxation term [26]. The value measured for the Kr-N_2 cell is $T_1 = 1.0(1)\,\mathrm{ms}$, while for the Ar-$N_2$ cell is $T_1 = 1.7(2)\,\mathrm{ms}$, when the two cells temperatures are set to the BG shift inversion point (331 K and 338 K respectively).

Estimating the coherence relaxation time T_2 is less straightforward since we have direct access only to the atomic populations. Nevertheless, we can deduce if T_2 is bigger or smaller than T_1 by looking at the shape of the Ramsey fringes. It is easy to show [27] that the Ramsey fringes envelope has positive concavity if $T_1 < T_2$ and negative concavity in the opposite case. Two Ramsey fringe patterns, taken at the same temperature of 335 K, are reported in Fig. 5 for the two cells examined. It can be observed that in the case of Kr-N_2 BG, the concavity is pronounced, indicating a value of T_2 shorter than 1 ms, whilst in the case of the Ar-N_2 cell, the concavity is much less evident, indicating a value of T_2 slightly shorter than T_1. This difference is expected because of the relaxation of the hyperfine coherence due to Van der Waals molecule formation between Kr and Rb [2,16,28], but it was not quantified in the design phase due to the lack of data in the literature for the pressure range of interest.

Having an experimental estimate of T_2 is important to define the optimal clock timings (in particular the Ramsey time). One way to obtain this parameter is to look at the contrast (C) of the central Ramsey fringe. Indeed, for small microwave detuning from center of the atomic resonance ($\Delta\nu \ll 1/t_1$), the envelope of the Ramsey fringes depends with a good approximation only on the coherence relaxation time T_2 [27]. We can thus look at the contrast of the central Ramsey fringe and approximate the behavior of this parameter as a function of the free-evolution time T with a single exponential, as:

$$C(T) = C_0 \exp\left\{-\frac{T}{T_2}\right\} \tag{7}$$

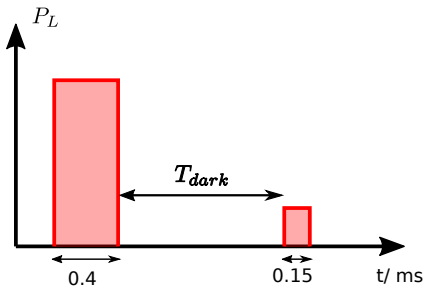

Figure 4: Timing sequence for the Franzen method.

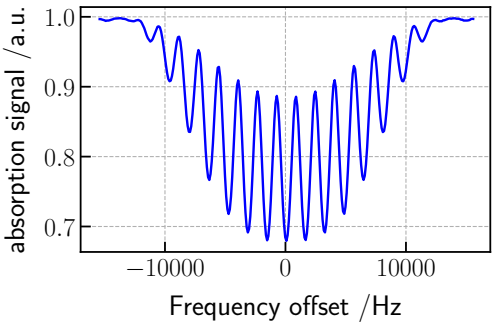

(a) Kr-N_2 Ramsey fringes. Rabi pulse duration $t_1 = 60\,\mu\mathrm{s}$, free-evolution time $T = 0.5\,\mathrm{ms}$.

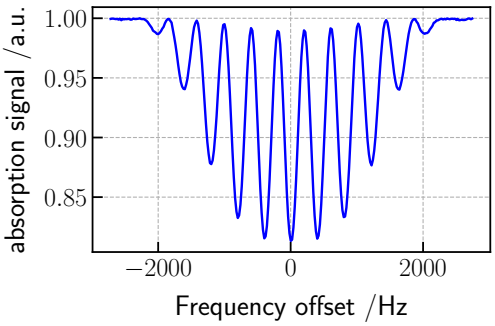

(b) Ar-N_2 Ramsey fringes. Rabi pulse duration $t_1 = 0.4\,\mathrm{ms}$, free-evolution time $T = 2\,\mathrm{ms}$.

Figure 5: Ramsey fringes of the clock transition for the two systems, obtained at the same temperature (335 K).

A typical set of data obtained with this procedure is shown in Fig. 6. At an operational temperature of 333 K we estimate a coherence relaxation rate $T_2 = 0.8(2)\,\mathrm{ms}$. This value suggests a Ramsey time of the same magnitude and a total clock cycle time close to 1 ms, still within the electronics capabilities of our digital control system.

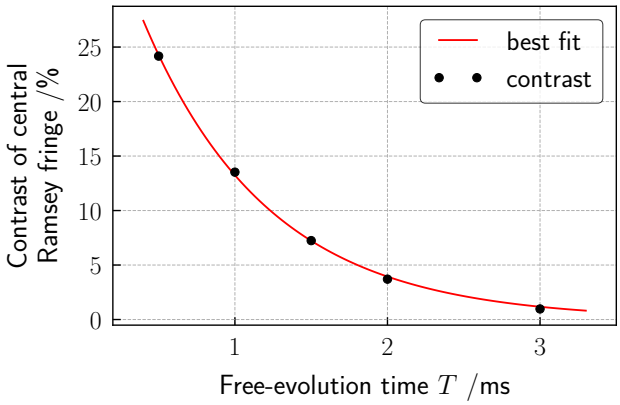

Figure 6: Typical exponential decay of the central fringe contrast as a function of the free-evolution time T. The figure refers to the Kr-N_2 cell.

In Fig. 7 we report the preliminary short-term stability of the POP clock operating with the Kr-N_2 mixture. The stability has been measured with the same timing adopted in Fig. 5a, but at a temperature corresponding to the inversion-point (331 K). The Allan deviation is $\sigma_y(\tau) = 8.7 \times 10^{-13}\,\tau^{-1/2}$. The same clock operating with the Ar-N_2 mixture showed a short-term stability around $4 \times 10^{-13}\,\tau^{-1/2}$. For both cells, the long-term behavior and the full metrological characterization will be the subject of a following work. We point out that the stability of the Kr-N_2 system is still $< 1 \times 10^{-12}\tau^{-1/2}$, a value still compatible with most of the practical applications and with potential benefit for the long-term performance due to the reduced absolute shift.

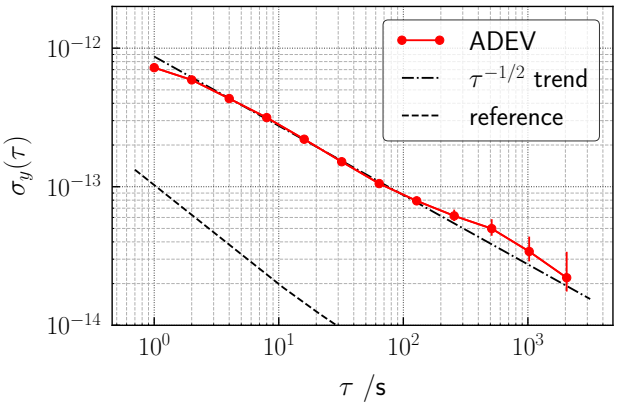

Figure 7: POP clock short term stability obtained with the Kr-N_2 mixture (Ramsey time 0.5 ms, cell temperature 331 K). The measurement bandwidth is 1 Hz and the reference oscillator is an active H-maser.

III. Conclusions

In previous works we have demonstrated that POP clock exhibits very good performances in term of both short- and long-term frequency stability in laboratory environment. In this work, we show that a novel mixture of BG, based on Kr and N_2, can be properly engineered to achieve a small BG-induced shift and at the same time obtain an inversion point as a function of temperature for the same shift. This is expected to reduce the clock sensitivity to two environmental parameters, i.e. pressure and temperature, at the same time.

With a pressure ratio around 0.9, moderate degradation of the short-term stability (compared to the traditional Ar-N_2 BG mixture) is obtained for a clock based on a centimeter-scale cell. Moreover, the BG-shift inversion temperature is maintained around 333 K, a good compromise to have a high-contrast signal together with reasonable power consumption. Even if the physics of the Rb-Kr collision needs to be investigate further, together with the long-term behavior of the clock, from the results reported in this paper it is quite evident that the shorter relaxation rates caused by the use of Kr do not seriously impair the clock stability, making it fully adequate to a large variety of scientific and industrial applications. Indeed, it is expected that the much lower frequency shift induced by the Kr-N_2 mixture will relax the specifications on the mechanical and thermal designs and allow a Rb clock to operate in environments characterized by large temperature and/or pressure drifts.

Acknowledgments

The authors acknowledge support from the GSTP contract GSTP6.2 AO7935: *Rb POP Atomic Clock* funded by the European Space Agency. We also thank Frequency Electronics Inc. (Long Island, NY) for providing us the Rb clock cell filled with the krypton mixture.

References

[1] J. Vanier and C. Audoin, *The Quantum Physics of Atomic Frequency Standards*. Philadelphia: Adam Hilger, 1989, vol. 2.

[2] W. Happer, "Optical pumping," *Rev. Mod. Phys.*, vol. 44, no. 2, pp. 169–249, apr 1972.

[3] J. Vanier, R. Kunski, N. Cyr, J. Y. Savard, and M. Têtu, "On hyperfine frequency shifts caused by buffer gases: Application to the optically pumped passive rubidium frequency standard," *J. Appl. Phys.*, vol. 53, no. 8, pp. 5387–5391, 1982.

[4] G. Missout and J. Vanier, "Pressure and temperature coefficients of the more commonly used buffer gases in rubidium vapor frequency standards," *IEEE Trans. Instrum. Meas.*, vol. 24, no. 2, pp. 180–184, June 1975.

[5] B. Bean and R. Lambert, "Temperature dependence of hyperfine density shifts. IV. ^{23}Na, ^{39}K, and ^{85}Rb in He, Ne, Ar, and N_2 at low temperatures," *Phys. Rev. A*, vol. 13, no. 1, p. 492, 1976.

[6] V. V. Batygin and V. S. Zholnerov, "Temperature dependence of the hyperfine transition frequency of the ground state of ^{87}Rb in a buffer medium," *Opt. Spectrosc.*, vol. 39, pp. 254–255, 1975.

[7] N. Cyr, Ph.D. dissertation, Universite Laval, Quebec (unpublished), 1983.

[8] P. L. Bender, E. C. Beaty, and A. R. Chi, "Optical detection of narrow ^{87}Rb hyperfine absorption lines," *Phys. Rev. Lett.*, vol. 1, no. 9, pp. 311–313, nov 1958.

[9] M. Huang, C. M. Klimcak, and J. C. Camparo, "Vapor-cell clock frequency and environmental pressure: Resonance-cell volume changes," in *2010 IEEE International Frequency Control Symposium*. IEEE, jun 2010.

[10] W. Moreno, M. Pellaton, C. Affolderbach, and G. Mileti, "Barometric effect in vapor-cell atomic clocks," *IEEE Trans Ultrason , Ferroelectr , Freq Control*, vol. 65, no. 8, pp. 1500–1503, aug 2018.

[11] N. Almat, M. Gharavipour, W. Moreno, F. Gruet, C. Affolderbach, and G. Mileti, "Long-term stability analysis toward 10^{-14} level for a highly compact POP Rb cell atomic clock," *IEEE Trans. Ultrason., Ferroelectr., Freq. Control*, vol. 67, no. 1, pp. 207–216, jan 2020.

[12] C. E. Calosso, A. Godone, F. Levi, and S. Micalizio, "Enhanced temperature sensitivity in vapor-cell frequency standards," *IEEE Trans. Ultrason., Ferroelectr., Freq. Control*, vol. 59, no. 12, pp. 2646–2654, Dec. 2012.

[13] F. Gong, Y.-Y. Jau, and W. Happer, "Nonlinear pressure shifts of alkali-metal atoms in inert gases," *Phys. Rev. Lett.*, vol. 100, no. 23, p. 233002, 2008.

[14] B. H. McGuyer, T. Xia, Y.-Y. Jau, and W. Happer, "Hyperfine frequencies of ^{87}Rb and ^{133} Cs atoms in Xe gas," *Phys. Rev. A*, vol. 84, p. 030501, Sep 2011.

[15] J. Camparo, "Nonlinear collision shifts of the 0-0 hyperfine transition due to van der waals molecule formation," *AEROSPACE REPORT NO. TOR-2019-00771*, Dec 2018.

[16] M. A. Bouchiat, J. Brossel, and L. C. Pottier, "Evidence for Rb-rare-gas molecules from the relaxation of polarized Rb atoms in a rare gas. experimental results," *J. Chem. Phys.*, vol. 56, no. 7, pp. 3703–3714, 1972.

[17] S. Micalizio, A. Godone, F. Levi, and C. Calosso, "Medium-long term frequency stability of pulsed vapor cell clocks," *IEEE Trans. Ultrason., Ferroelectr., Freq. Control*, vol. 57, no. 7, pp. 1524–1534, July 2010.

[18] S. Micalizio, C. E. Calosso, A. Godone, and F. Levi, "Metrological characterization of the pulsed Rb clock with optical detection," *Metrologia*, vol. 49, no. 4, p. 425, 2012.

[19] M. D. Rotondaro and G. P. Perram, "Collisional broadening and shift of the rubidium D_1 and D_2 lines ($5^2S_{12} \rightarrow 5^2P_{12}$, 5^2P_{32}) by rare gases, H_2, D_2, N_2, CH_4 and CF_4," *J. Quant. Spectrosc. Radiat. Transfer*, vol. 57, no. 4, pp. 497 – 507, 1997.

[20] C. Ottinger, R. Scheps, G. W. York, and A. Gallagher, "Broadening of the Rb resonance lines by the noble gases," *Phys. Rev. A*, vol. 11, pp. 1815–1828, Jun 1975.

[21] B. François, C. E. Calosso, M. Abdel Hafiz, S. Micalizio, and R. Boudot, "Simple-design ultra-low phase noise microwave frequency synthesizers for high-performing Cs and Rb vapor-cell atomic clocks," *Rev. Sci. Instrum.*, vol. 86, no. 9, p. 094707, 2015.

[22] C. E. Calosso, S. Micalizio, A. Godone, E. K. Bertacco, and F. Levi, "Electronics for the pulsed rubidium clock: Design and characterization," *IEEE Trans. Ultrason., Ferroelectr., Freq. Control*, vol. 54, no. 9, pp. 1731–1740, September 2007.

[23] C. E. Calosso, M. Gozzelino, E. Bertacco, S. Micalizio, B. François, and P. Yun, "Generalized electronics for compact atomic clocks," in *2017 Joint Conference of the European Frequency and Time Forum and IEEE International Frequency Control Symposium (EFTF/IFCS)*, July 2017, pp. 322–323.

[24] W. Franzen, "Spin relaxation of optically aligned rubidium vapor," *Phys. Rev.*, vol. 115, no. 4, pp. 850–856, aug 1959.

[25] M. Gharavipour, C. Affolderbach, F. Gruet, I. S. Radojičić, A. J. Krmpot, B. M. Jelenković, and G. Mileti, "Optically-detected spin-echo method for relaxation times measurements in a Rb atomic vapor," *New J. Phys.*, vol. 19, no. 6, p. 063027, jun 2017.

[26] S. Micalizio, A. Godone, F. Levi, and J. Vanier, "Spin-exchange frequency shift in alkali-metal-vapor cell frequency standards," *Phys. Rev. A*, vol. 73, no. 3, mar 2006.

[27] S. Micalizio, C. E. Calosso, F. Levi, and A. Godone, "Ramsey-fringe shape in an alkali-metal vapor cell with buffer gas," *Phys. Rev. A*, vol. 88, no. 3, sep 2013.

[28] F. Hartmann and F. Hartmann-Boutron, "Shift and broadening of the ^{87}Rb 0-0 line due to collisions with krypton buffer-gas atoms," *Phys. Rev. A*, vol. 2, no. 5, pp. 1885–1892, nov 1970.